Additive White Gaussian Noise Level Estimation in SVD Domain for Images

Wei Liu and Weisi Lin, *Senior Member, IEEE*

***Abstract*— Accurate estimation of Gaussian noise level is of fundamental interest in a wide variety of vision and image processing applications as it is critical to the processing techniques that follow. In this paper, a new effective noise level estimation method is proposed on the basis of the study of singular values of noise-corrupted images. Two novel aspects of this paper address the major challenges in noise estimation: 1) the use of the tail of singular values for noise estimation to alleviate the influence of the signal on the data basis for the noise estimation process and 2) the addition of known noise to estimate the content-dependent parameter, so that the proposed scheme is adaptive to visual signals, thereby enabling a wider application scope of the proposed scheme. The analysis and experiment results demonstrate that the proposed algorithm can reliably infer noise levels and show robust behavior over a wide range of visual content and noise conditions, and that is outperforms relevant existing methods.**

***Index Terms*— Additive white Gaussian noise, noise estimation, singular value decomposition (SVD).**

I. Introduction

NOISE is unavoidable during visual data acquisition, processing and transmission, and often exhibits as the random variation of brightness or color in images. Possible sources of random noise include film grain [1]–[3], various sensors and circuits [4]–[6] of digital equipment (e.g., a scanner, digital camera, [7], [8] or photon detector [9]–[11]), signal quantization and communication channels. Denoising is therefore a very important step to improve the accuracy or performance of many image processing techniques, such as image segmentation [12], [13] and recognition [14], [15]. There has been a large body of literature on image denoising (e.g., [16]–[20]). Although very promising denoising results have been achieved using a variety of methods, such as wavelets, anisotropic diffusion and bilateral filtering, the noise level in the image is often assumed known or already estimated beforehand [16]–[18]. Different attempts for noise and artifact estimation have been performed [21]–[24]; the estimation of noise level is difficult in practice, and overall, noise estimation is a relatively less investigated issue in the literature (in comparison with the area of denoising). Apart from denoising, other algorithms that can benefit from noise level estimates include motion estimation [25], super-resolution [26], shape-from-shading [27], and feature extraction [28].

In most cases, noise can be modeled as Gaussian distribution, and such noise includes: 1) the amplifier noise of an image sensor [29]; 2) the shot noise of a photon detector, which is a type of electronic noise that may be dominant when a finite number of particles that carry energy is sufficiently small [9]–[11]; and 3) the grain noise of photographic film [1]–[3]. Estimating the Gaussian noise level from a single image is a difficult task: we need to decide whether local image variations are due to color, texture and lighting variations of the image itself, or due to the noise. In the image denoising literature, noise is often assumed to be zero-mean additive white Gaussian noise (AWGN) [30]. An observed noisy image $A(i, j)$ is expressed as:

$$A(i, j) = A_0(i, j) + N(i, j) \tag{1}$$

where $A_0(i,j)$ represents the original (true) image, and $N(i,j)$ signifies the signal-independent noise. The amplitude of noise is of Gaussian distribution:

$$f(x) = \frac{1}{\sigma\sqrt{2\pi}} e^{-\frac{(x-\mu)^2}{2\sigma^2}} \tag{2}$$

where σ represents the noise standard deviation and μ is the mean value of the distribution. For zero-mean AWGN (i.e., $\mu = 0$), the key parameter to be determined is only σ.

There are two major challenges in noise estimation from a single image: 1) how to prepare a data basis for noise level estimation with minimum influence of the image signal itself (otherwise, we would estimate noise based upon signal data) and 2) how to allow the algorithm adaptive to visual content so that it is suitable for different images. Noise estimation algorithms developed so far can be classified into three different approaches: filter- (or smoothing-) based, block-based and transform-based.

In filter-based methods [21], [31], a noisy image is first filtered by a low-pass filter to suppress the noise. Then the noise variance is computed from the difference between the noisy image and the filtered image. The main difficulty of filter-based methods in preparing the data basis is that the difference image is assumed to be the noise but this assumption is not held in general, because it is well known that a low-pass filtered image is not the original image, especially for an image with strong structure or other visual details. In order to get a data basis for noise level estimation with minimum influence of the image signal itself, in [31], the vertical and

Manuscript received August 12, 2011; revised August 26, 2012; accepted September 2, 2012. Date of publication September 18, 2012; date of current version January 24, 2013. This work was supported in part by the Singapore Ministry of Education Academic Research Fund Tier 2 under Grant T208B1218. The associate editor coordinating the review of this manuscript and approving it for publication was Prof. Hsueh-Ming Hang.

W. Liu is with the School of Computer Science, South China Normal University, Guangzhou 510631, China (e-mail: beebearbb@hotmail.com).

W. Lin is with the School of Computer Engineering, Nanyang Technological University, 639798 Singapore (e-mail: wslin@ntu.edu.sg).

Color versions of one or more of the figures in this paper are available online at http://ieeexplore.ieee.org.

Digital Object Identifier 10.1109/TIP.2012.2219544

horizontal information of an image is used for extracting vertical/horizontal detail components and histogram information for noise estimation, but it has a high computational load and a number of user-defined parameters to determine.

In blocked-based methods [22], [32], images are tessellated into a number of blocks. The noise variance is then computed from a set of homogeneous blocks. The main assumption here is that a homogeneous block in an image is a result of an absolutely smooth image block with added noise. In fact, homogeneity is a relative condition in real-world images, and a relatively homogeneous block has a big chance to contain some visual activities there. Another issue of block-based methods is how to identify the homogeneous blocks with model parameters suitable for images in general.

There have been modified filter-based [31], [33] and block-based approaches [34], [35] for better noise estimation. Generally, block-based algorithms are simple, but their estimates may vary significantly depending on the input image and noise level. Filter-based algorithms yield good estimates for large noise cases, but they require a high computational load and a large amount of memory. There have some compromised methods as the combination of filter-based and block-based estimation algorithms [36]–[38].

Among transform-based methods, a widely used estimation method is based on mean absolute deviation (MAD) [23], [39]. The estimation of noise standard deviation σ is formulated as follows:

$$\hat{\sigma}_n = \frac{median(|y_i|)}{0.6745}, \qquad y_i \in subband\ HH \tag{3}$$

where *HH* denotes the diagonal band in wavelet decomposition, y_i denotes the coefficients in the diagonal band, and $median(\cdot)$ represents the median operation. The approach is based on the assumption that wavelet coefficients in the *HH* subband are dominated by noise. In practice, the outcome achieved by this approach is usually higher than the truth value; the reason is that coefficients in *HH* subband are dominated not only by noise, but also by image details. The number of coefficients contributed by image details is few, but usually takes on big magnitude, which results in the greater outcome achieved by the median of all coefficients in *HH* subband. In the case where the resultant data basis for estimation contains more image details and less noise, the estimation is less accurate. Some modified algorithms have been proposed based on the coefficients estimation of the original image in the *HH* subband [40]. In [40], better results can be obtained by deducting the estimated original image contribution from *HH*; then the estimation is performed based on the Donoho's formula as shown in (3).

To address the two aforementioned major challenges and overcome the drawbacks in the existing work, we investigate into the possibility to estimate noise in singular value decomposition (SVD) domain. The SVD has been successfully applied to many image restoration [41]–[46] and recognition [47]–[49] problems. As to be analyzed in the next section, the remarkable property of the SVD is its statistical representations of image details in subspaces of decreasing importance, while the influence of noise maintains in all subspaces. This fact is helpful since the tail of singular values (i.e., the later SVD subspaces) can be used as the proper data basis for noise estimation and image details do not have significant influence in that part of subspaces. In essence, the use of SVD enables separation of image details and noise in a single image and such separation is difficult otherwise.

To be more specific in analysis, we divide "the singular" values S of a noise-corrupted image into two parts in SVD — S_s and S_n, where S_s denotes the part contributed by image structure and S_n denotes the part contributed by noise (we will explain how to calculate S_s and S_n in Section II). We did abundant experiments. Figure 1 shows experimental result of the Lena image of different sizes for S_s and S_n, with different noise injection. We can see that image details contribute very little to the later part of the singular values, as S_s; on the contrary, noise dominates the later part of the singular values, as S_n. When noise level (σ) become lower, the contribution of noise will be smaller either; however, the tail of the singular values is still dominated by noise. The figure shows the best dada basis (i.e., the range of singular values) for noise estimation is the later 80% of singular values, because this represents the data to which noise is the dominant factor. It is worthy of being noted that the influence of signal decreases rapidly in S, so the possible data basis for noise estimation can be as large as 80% of S – a bigger amount of data facilitates more reliable noise estimation.

In the work to be presented next in more details, we will firstly study the characteristics of singular values of noise-degraded images (as Section II) and propose a new method of noise level estimation in the SVD domain for AWGN (as Section III) accordingly, to better address the two major challenges that we have discussed. The experiments on different types of images demonstrate that the proposed algorithm can reliably detect Gaussian noise levels and show robust behavior over a wide range of visual content and noise conditions, in Section IV. The conclusion for the work will be in Section V.

II. SVD for Images and the Influence of AWGN

A. Singular Values and Noise Levels

The SVD is based on the theory in linear algebra with which a rectangular matrix A can be decomposed into the product of three matrices - an orthogonal matrix U, a diagonal matrix S, and the transpose of another orthogonal matrix V. To be more specific, the SVD of an $m \times n$ image $\boldsymbol{A}$ (assume r is the rank of A) can be written as:

$$A = U \times S \times V^T \tag{4}$$

where $U^T U = I_{mm}$; $V^T V = I_{nn}$ (I_{mm} and I_{nn} denote the m-square and n-square identity matrices); m and n represent the dimensions of A. The columns of U are orthonormal eigenvectors of AA^T, the columns of V are orthonormal eigenvectors of $A^T A$, and S is a diagonal matrix containing the square roots of eigenvalues of AA^T or $A^T A$ arranged in the descending order. Let the singular values be denoted by $s(i)(i = 0, 1, \ldots, r)$, and then $s(1) > s(2) > \cdots > \cdots > s(r)$.

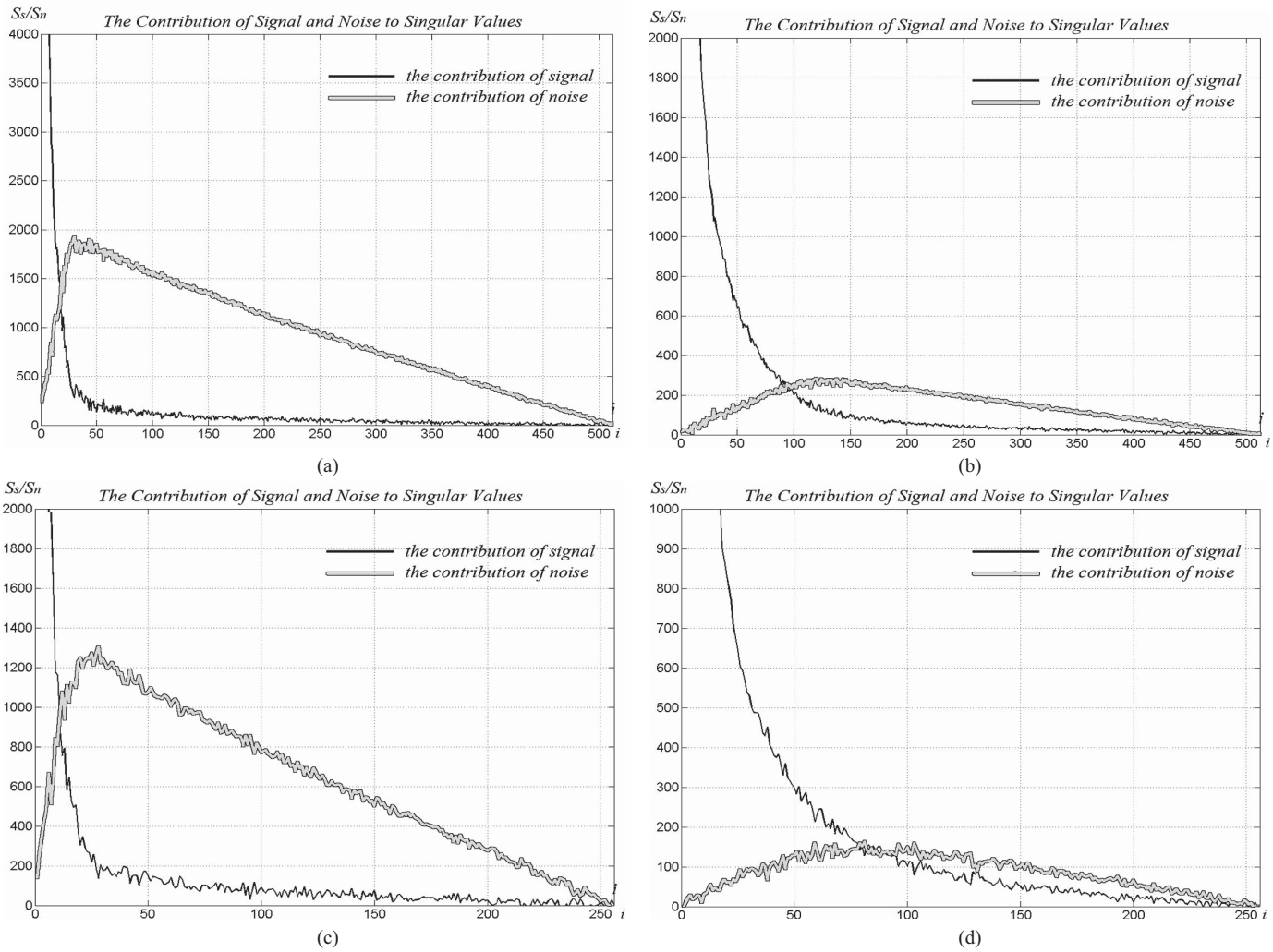

Fig. 1. Contribution of signal and noise to singular values. (a) *Lena* 512×512, $\sigma = 50$. (b) *Lena* 512×512, $\sigma = 10$. (c) *Lena* 256×256, $\sigma = 50$. (d) *Lena* 256×256, $\sigma = 10$.

To separate the contribution of image from that of noise, following the notations in the last section (Equation (1)), S_s and S_n are defined as the singular values due to the original image and the additive noise decomposed by singular vectors U and V:

$$S_s = U^{-1} \times A_0 \times (V^T)^{-1} = U^T \times A_0 \times V \tag{5}$$

$$S_n = U^{-1} \times N \times (V^T)^{-1} = U^T \times N \times V. \tag{6}$$

Obviously $S = S_s + S_n$, or $s(i) = s_s(i) + s_n(i)$.

Figure 2 shows singular values $s(i)$ of different test images with different noise levels. In Figure 2, (a), (b) and (c) are three standard 512×512 grayscale test images; (d) is a standard 256×256 grayscale test image; (e) is a 256×256 cartoon image; (f) is a 533×512 cartoon image. We can see that addition of noise to images increases the singular values in general (in line with what has been shown in Figure 1), and this is also agreeable with the results in [50]. In other words, the higher the noise level is, the larger the singular values become. More importantly, the early part of singular values (when i is small) are determined mainly by the image content (noise is there also but its influence is insignificant due to the strong presence from the signal itself), while the noise level can be distinguished much easily with the later part (i.e., the tail) of singular values (when i is large). This is the ground of the proposed technique in this paper for noise estimation.

B. AWGN Analysis

Let N be a zero-mean m×n AWGN image with standard deviation σ, and its SVD can be expressed as:

$$N = U \times S_n \times V^T \tag{7}$$

and

$$\sigma^2 = \sum_{i=1}^{r} s_n^2(i).$$

We use parameter M to represent the number of the last singular values (i.e., the tail) under consideration. Obviously, the average of the last M singular values is a function of σ, and can calculated as

$$P_M(\sigma) = \frac{1}{M} \sum_{i=r-M+1}^{r} s_n(i) \tag{8}$$

where $1 \leq M \leq r$. When $M = 1$, only the last singular value (i.e., $s_n(r)$) is considered in (8); when $M = r$, all singular values (i.e., $s_n(1)$ to $s_n(r)$) are considered in (8).

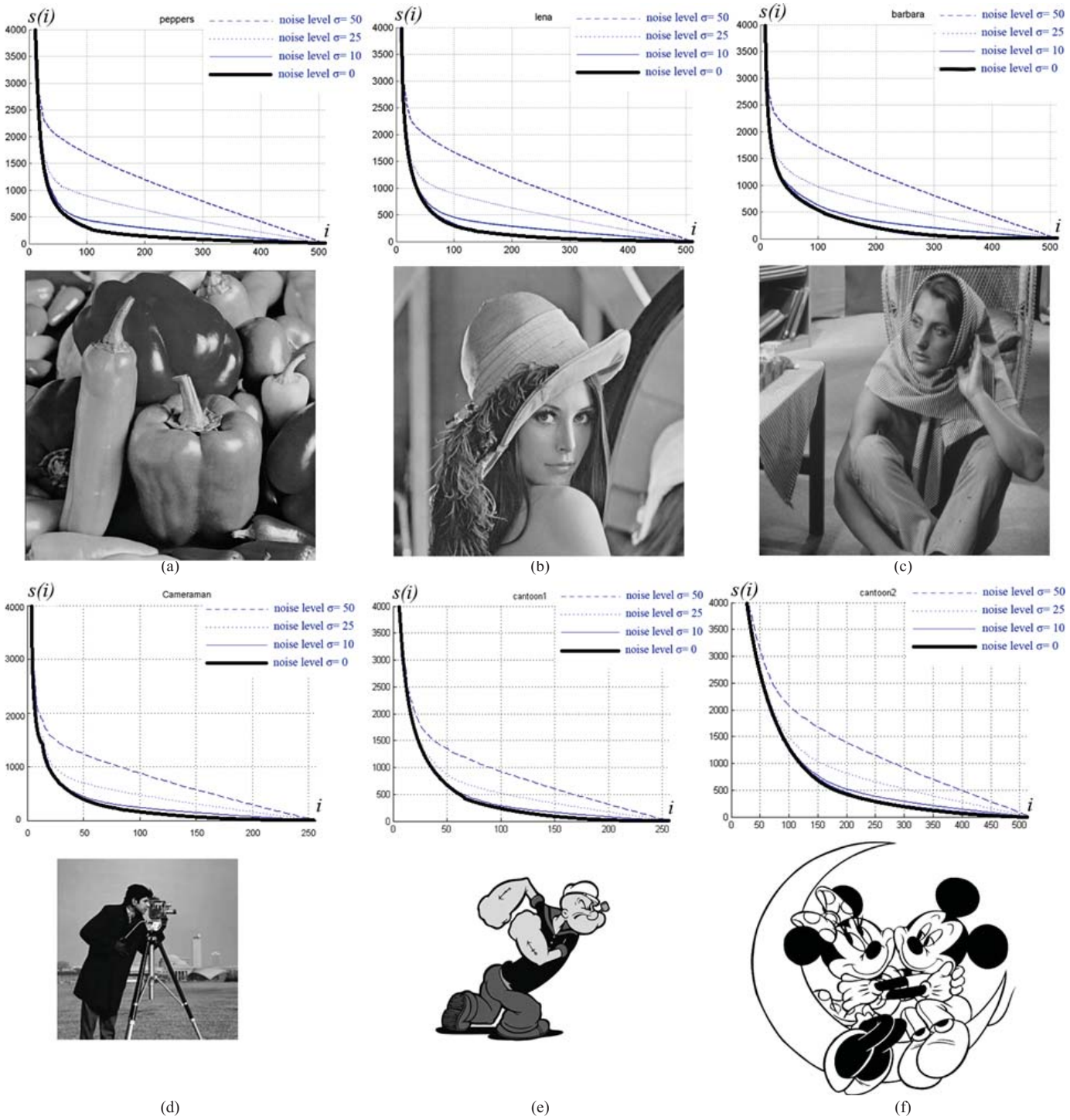

Fig. 2. Singular values of different test images with different noise levels. (a) Singular values of *Peppers* (512 × 512). (b) Singular values of *Lena* (512 × 512). (c) Singular values of *Barbara* (512 × 512). (d) Singular values of *Cameraman* (256 × 256). (e) Singular values of image (256 × 256). (f) Singular values of image (533 × 512).

If P_M is linearly dependent on σ, two sufficient and necessary conditions must be satisfied:

$$\begin{cases} P_M(k\sigma) = k \times P_M(\sigma) \\ P_M(\sigma + \sigma_1) = P_M(\sigma) + P_M(\sigma_1) \end{cases} \tag{9}$$

where σ represents the standard deviation of an additional noise N_1.

Let us look at the first condition in (9) first. Assume $N_k = k \times N$ to be an $m \times n$ AWGN image from the same process of N : N_k is a modified version (i.e., an amplified or reduced version, depending on k) of N; that is, N and N_k are formed by a same AWGN process. The resultant standard deviation will be $k \times \sigma$, and we have

$$\begin{aligned} N_k = k \times N = k \times U \times S_n \times V^T = U \times kS_n \times V \\ = U \times S_{kn} \times V^T \end{aligned} \tag{10}$$

TABLE I
RELATIONSHIP OF P_M AND α FOR AWGN WITH DIFFERENT IMAGE SIZES OF THE DIFFERENT PROCESSES ($M = 3R/4$) FOR DETERMINING α

	$\sigma = 10$	$\sigma = 15$	$\sigma = 20$	$\sigma = 25$	$\sigma = 30$	$\sigma = 35$	$\sigma = 40$	$\sigma = 45$	$\sigma = 50$	α
P_M (512 × 512)	138.40	207.49	276.41	346.53	416.16	485.18	553.71	623.92	693.38	13.87
P_M (256 × 256)	98.26	148.22	196.56	247.46	294.55	346.18	393.11	444.47	489.75	9.83
P_M (128 × 128)	70.05	104.11	140.17	177.02	211.35	248.19	281.03	318.74	348.99	7.02

where

$$S_{kn} = k \times S_n. \tag{11}$$

Therefore,

$$P_M(k\sigma) = \frac{1}{M}\sum_{i=r-M+1}^{r} k s_n(i) = k \times P_M(\sigma). \tag{12}$$

Equation (12) shows that the first condition in (9) is satisfied when the noise is from the same process.

Let $N_1 = (\sigma_1/\sigma)\times N$ be an $m\times n$ AWGN image of the same process of N with standard deviation σ_1, and $N_2 = N_1 + N = \frac{\sigma_1+\sigma}{\sigma}N$ be an $m \times n$ AWGN image of the same process of N with standard deviation $(\sigma + \sigma_1)$. We have

$$\begin{aligned} N_1 &= \frac{\sigma_1}{\sigma}N = \frac{\sigma_1}{\sigma}U \times S_n \times V^T = U \times \frac{\sigma_1}{\sigma}S_n \times V^T \\ &= U \times S_{1n} \times V^T \end{aligned} \tag{13}$$

$$S_{1n} = \frac{\sigma_1}{\sigma}S_n \tag{14}$$

$$\begin{aligned} N_2 &= \frac{\sigma+\sigma_1}{\sigma}N \\ &= \frac{\sigma+\sigma_1}{\sigma}U \times S_n \times V^T \\ &= U \times \frac{\sigma+\sigma_1}{\sigma}S_n \times V^T \\ &= U \times S_{2n} \times V^T \end{aligned} \tag{15}$$

So,

$$S_{2n} = \frac{\sigma+\sigma_1}{\sigma}S_n \tag{16}$$

$$\begin{aligned} P_M(\sigma+\sigma_1) &= \frac{1}{M}\sum_{i=r-M+1}^{r}\frac{\sigma+\sigma_1}{\sigma}s_n(i) \\ &= \frac{1}{M}\sum_{i=r-M+1}^{r} s_n(i) + \frac{1}{M}\sum_{i=r-M+1}^{r}\frac{\sigma_1}{\sigma}s_n(i) \\ &= P_M(\sigma) + P_M(\sigma_1). \end{aligned} \tag{17}$$

Equation (17) shows that the second condition in (9) is satisfied when the noise is from the same process. From (12) and (17) we can see that P_M is linearly dependent on the noise level σ if the process of AWGN is the same.

In the case of different processes of AWGN (e.g., we use the randn( ) function in Matlab to generate an AWGN sequence N of standard deviation σ, and then randn( ) is used again to generate another AWGN sequence N_1 of standard deviation σ_1, i.e., N_1 is not an amplified or reduced version of N), P_M is no longer linearly dependent on σ for any M value. The extensive experimental results confirm that P_M of a noise from a different process behaves almost the same as the case of noise with same processes (as presented above in this section) when M is significantly bigger than 1, and Table I shows some examples for P_M versus σ, with different image sizes. That is, P_M is almost linearly dependent on the noise level σ even if the process of AWGN changes:

$$P_M(\sigma) = \alpha\sigma \quad \text{when} \quad M >> 1 \tag{18}$$

where α denotes the slope of the linear function which can be affected by the choice of M. If $M < r/4$, the randomness of AWGN will cause the value of P_M vibrated. In our experiments on 512×512 AWGN images, we calculate P_M as the average of the $128^{\text{th}} \sim 512^{\text{th}}$ singular values. Thus we can figure out that from the experiments data shown in Table I. With change of the process of AWGN, the value of α changes slightly; we have for 512×512 images.

With the images of cartoons and real-world scenes, the average of the last M singular values P_M is calculated, and we find that the relationship between P_M and σ become:

$$P_M = \sum_{i=r-M+1}^{r} S_i = \alpha\sigma + \beta. \tag{19}$$

In comparison with (18) and (19), we know that β is image content related. We can also separate P_M into two parts—P_{Ms} and P_{Mn}, for signal and noise respectively, and they are defined as

$$P_{Ms} = \sum_{i=r-M+1}^{r} S_s(i) \tag{20}$$

$$P_{Mn} = \sum_{i=r-M+1}^{r} S_n(i) \tag{21}$$

where P_{Ms} denotes the contribution of image structures to P_M, and P_{Mn} denotes the contribution of noise to P_M.

Figures 3 and 4 take 512×512 noise-corrupted Lena image as an example and show the experimental results. In Figure 3, $M = 384$. We can see that the line of P_{Mn} is almost the same as that of pure AWGN. The line of P_{Ms} is almost horizontal, i.e., P_{Ms} is a constant. This is agreeable with (19), where PM is the sum of $\alpha\sigma$ and β, $\alpha\sigma$ is the contribution from noise and constant β is the contribution from image structure. The more complex an image is, the greater the value of β is. Figure 4 shows the relationship of P_{Mn} and M at different noise levels. We can also see from Figure 1, the tail of S_n changes according to noise level. When noise level is low, the tail where noise is dominant is short; when noise level is high, the tail is long.

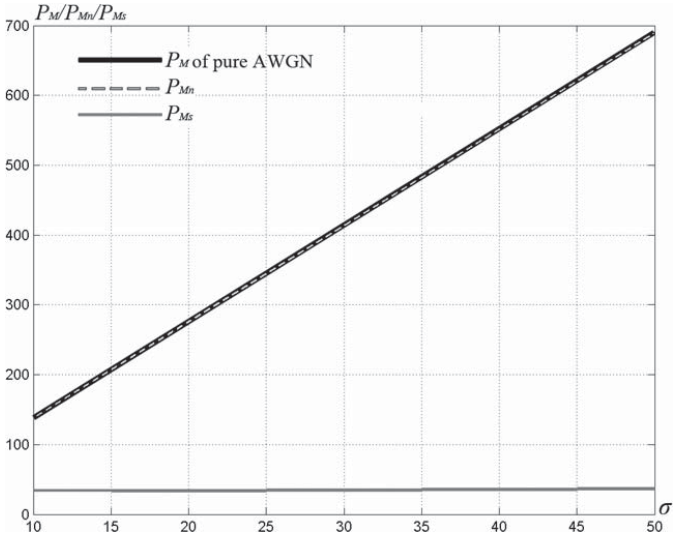

Fig. 3. Contribution of signal and noise to P_M.

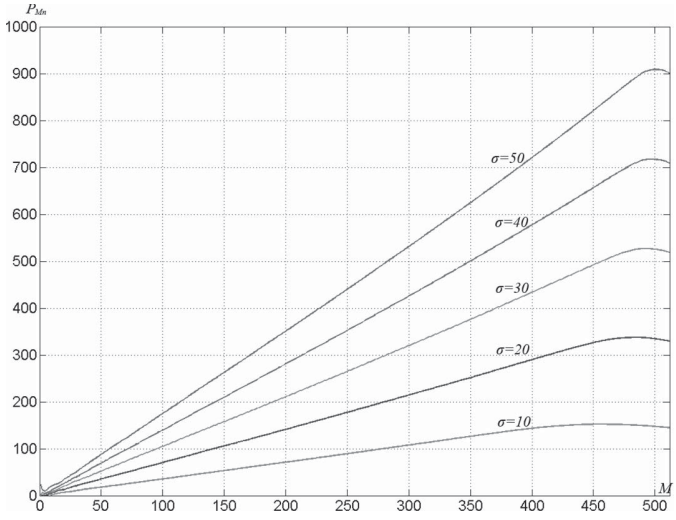

Fig. 4. Relationship of P_{Mn} and M.

When we decide the value of M, we should not use a too-large M because it would cause the inclusion of the early part of singular values into the calculation for P_M (this is obvious from Equations 8, 12, 17, 19–21), and we have known that the image content dominates the early part of singular values-bear in mind that we are to use singular values to estimate noise; so M should be no larger than $\frac{4r}{5}$. On the other hand, M should not be too small either since this would cause the data size for noise estimation too small and therefore affecting the estimation accuracy and reliability; as discussed before, M should be larger than or equal to $\frac{r}{4}$. In summary, the range of M should be $M \in \left[\frac{r}{4}, \frac{4r}{5}\right]$; as can be seen (also to be further demonstrated later in Figure 6), the M value selection is not critical since the range is wide (because r is sufficiently large for images).

Figure 5 gives some experimental results of different kinds and sizes of images ($M = 3r/4$), where the X axis denotes the noise level and Y axis denotes P_M. Fig. 5(a) shows the experimental results from standard 512×512 grayscale test images. From the top to the bottom, the curves correspond to Barbara, Peppers, Lena and a blank image (the two curves corresponding to Lena and Peppers almost overlap). We test a blank image in order to find the relation of PM and noise level without the influence of image content. Fig. 5(b) illustrates the experimental results from 256×256 images including those in Fig. 2(d) and Fig. 2(e). The bottom one is a 256×256 blank image. We can see from Fig. 5(b) that the curves of the same size images are also linear and parallel. Fig. 5(c) shows the experimental results from 533×512 Cartoon2. We find that the curve corresponding to Cartoon2 is also parallel to the curve of blank images of the same size. From Fig. 5 (a, b, c) we can see that PM is linearly dependent on the noise level under all these circumstances. Image details have little influence on slope α, but can increase β notably. In other words, image structures and details contribute to the value of β. Generally, for images with more details, the value of β is greater. We can see that Barbara has the largest β among all the standard 512×512 grayscale test images in Figure 2.

We also perform experiments for the relationship between M and α. The experimental results on 512×512 images are shown in Figure 6. With the increase of M, the value of α increases. The value of P_M is still linearly related to the noise level with slope of α approximately. As we mentioned above, if M is too larger, i.e., $M > 448$ in this case, the relation of P_M and α may not be linear any more (see the last row of plots in Figure 6); if M is too small, i.e., $M < 128$, the value of P_M may be vibrated (as the first row of plots in Figure 6). Fortunately, the range for M is sufficiently large.

III. Proposed Noise Estimation Algorithm in the SVD Domain

The experimental results and analysis we described in Section II show the relation of the average of the last M singular values (i.e., P_M) and the AWGN level (i.e., σ) is of approximate linearity. That is, P_M and σ follow the relation expressed in (19). This provides the ground for noise estimation.

For various images, as has been shown in the previous section, if a not-extreme (i.e., not to be very small or large) M value is selected, the slope parameter α is almost the same for images of the same size. That is to say, for images of the same size, M is the only factor affect the value of α. For instance, if $M = 384$ (i.e., $3r/4$) for 512×512 images, according to the statistics from the same size pure AWGN image of different noise level, the value of α is 13.87 as shown in Table I; if $M = 192$ (also $3r/4$) for 256×256 images, the value of α is 9.83 (as in Table I). In this work, we choose $M = 3r/4$; as we mentioned earlier, any choice in the range of $(\frac{r}{4}, \frac{4r}{5})$ is reasonable. For images of other size, we can determine α as following steps.

1) Calculate PM of pure AWGN images of the same size at different noise levels, we get a set of data like a row in Table I.
2) Calculate α by the least square fitting according to data acquired in the first step.

In practical, since α is independent of image content, we can figure out α off-line. For example, most digital image capture

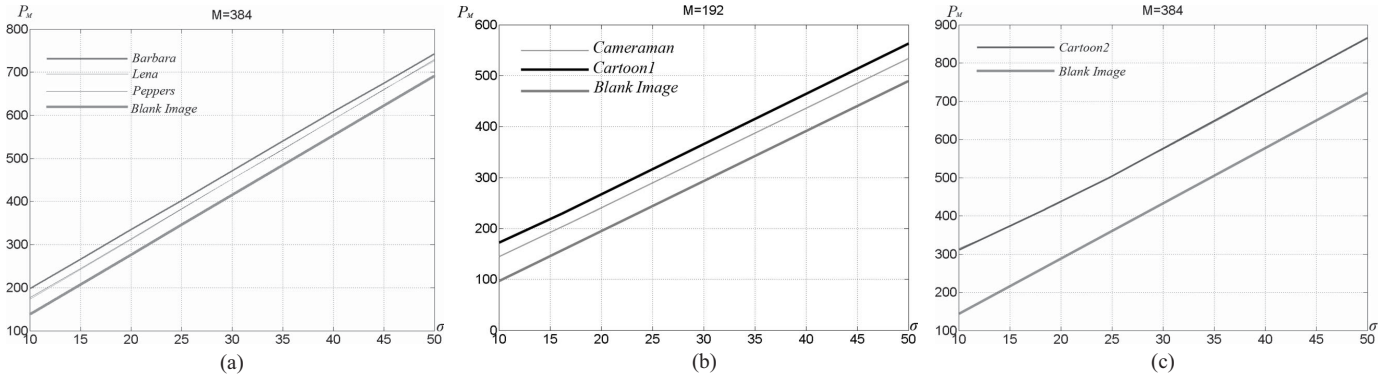

Fig. 5. Relationship of PM and σ. (a) 512×512 standard gray images. (b) 256×256 images. (c) 533×512 Cartoon2.

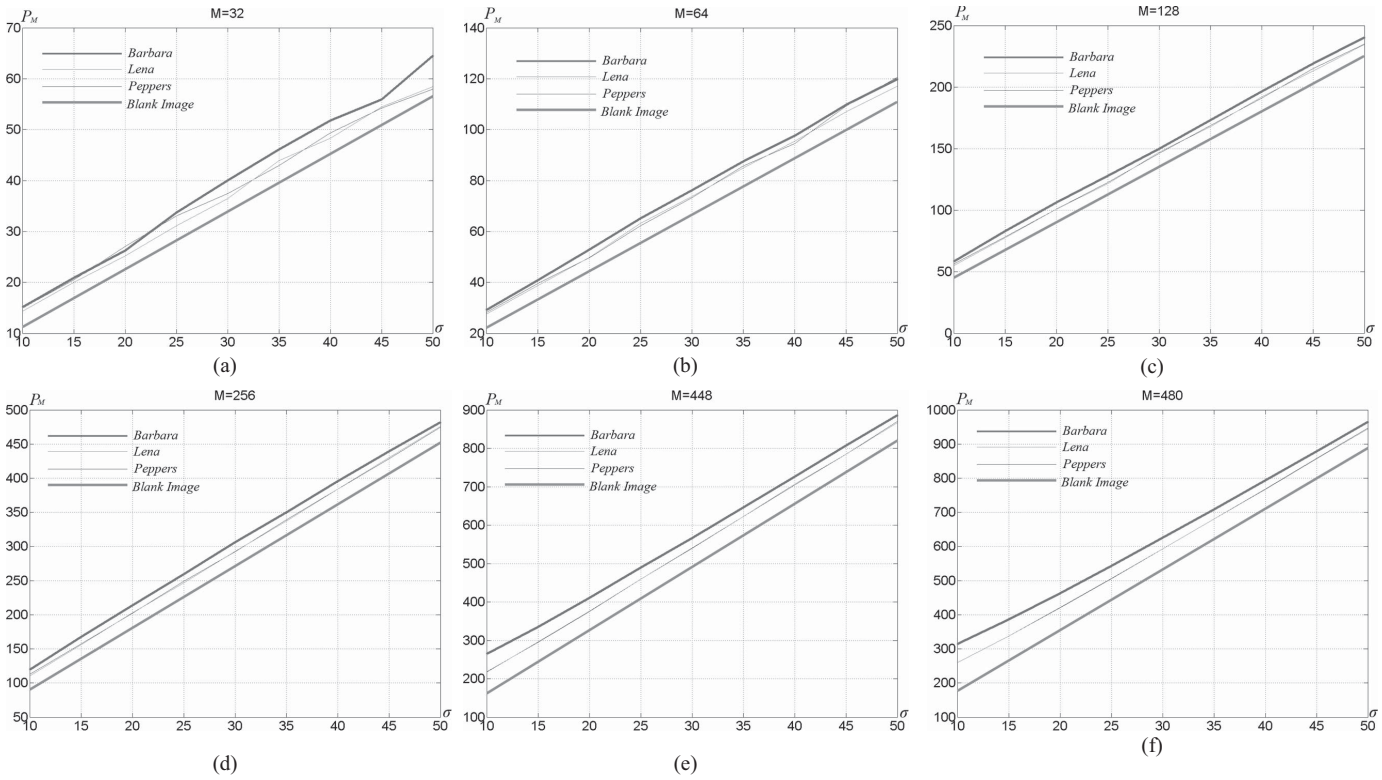

Fig. 6. Relationship between M and α.

equipment can only acquire images of several fixed size. We can calculate α corresponding to each image size, and form a table for the relation between image size and α beforehand.

When we estimate noise level σ according to Equation (19), we need to find out the value of β. As we mentioned in Section II, β is related to the complexity (structures and other visual details) of the image, but it is hard to find out the precise value for β. To solve the problem, we propose to add additional AWGN with known deviation to the noise-corrupted image, and let the outcome tell us the value of β.

Assume that the noise deviation is σ in the input noise-corrupted image. If we add known AWGN of σ_1 to the noise-corrupted image, then it is easy to illustrate (see below) that the total noise σ_2 will still be AWGN with standard deviation of $\sqrt{\sigma^2 + \sigma_1{}^2}$.

We only need to consider the influence from the noise since, as we already demonstrated, P_M with a proper M is mainly affected by noise. Assume that N is the AWGN sequence with deviation σ, and N_1 is the AWGN sequence that we added to the noised image. For zero mean AWGN, the mean values are zero, i.e., $E(N) = 0$ and $E(N_1) = 0$

$$\sigma^2 = E[N - E(N)]^2 = EN^2 \tag{22}$$

$$\sigma_1^2 = E[N_1 - E|(N_1)]^2 = E(N_1^2). \tag{23}$$

The variance of total noise:

$$\begin{aligned} \sigma_2^2 &= E[(N + N_1) - E(N + N1)]^2 \\ &= E(N^2) + E(N_1^2) + 2E(NN_1) \\ &= E(N^2 + E(N_1^2) \\ &= \sigma^2 + \sigma_1^2. \end{aligned} \tag{24}$$

Noted, N and N_1 are not related, and this means that $E(NN_1) = E(N)E(N_1) = 0$. Thus we can get

Equation (24), and we can calculate the standard deviation σ_2 as:

$$\sigma_2 = \sqrt{\sigma^2 + {\sigma_1}^2} \tag{25}$$

We have two equations with two variable, β and σ from (19):

$$P_M = \alpha\sigma + \beta \tag{26}$$

$$P_{1M} = \alpha\sqrt{\sigma^2 + {\sigma_1}^2} + \beta. \tag{27}$$

Since β is a content-dependent parameter, it is derived by adding noise to the test image each time when we estimate the AGWN level. This is one of the innovative points in our work, we do not derive β based upon simulation with a group of images (it is difficult since we would end up with the need to classify/estimate the image content in order to determine β); instead, we add known noise to the image under test every time to obtain two noising image versions of same content to derive β. So the above equation set is applicable to all kinds of images. The simulation results in Part IV also proved the efficiency of our technique has little to do with the content of images.

Solving the equation set above, we can figure out the value of σ

$$\hat{\sigma} = \frac{\alpha\sigma_1^2}{2(P_{1M} - P_M)} - \frac{P_{1M} - P_M}{2\alpha} \tag{28}$$

Theoretically, σ_1 of the added AWGN can be arbitrary. In practice, the choice of σ_1 affects the precision of estimation. If σ_1 is too small, according to (25), the total noise level σ_2 will be too close to σ, i.e., the two points $-(\sigma_1, P)$ and (σ_2, P_1) will be too close, as illustrated as Point B in Figure 7, which is too close to the Target Point A; this affects the precision and stability of the estimation result. It will be beneficial to choose a bigger value of σ_1; for example, Point C in Figure 7 is better than Point B. In our experiments, we choose $\sigma_1 = 50$

The proposed noise level estimation procedure for image A is therefore composed of 7 stages as follows:

1) Choose a proper M (the suggested M value is $r \times 3/4$), and calculate corresponding α;
2) Perform singular value decomposition to the noised image A;
3) Calculate the average of the last M singular values P_M;
4) Add AWGN of $\sigma_1 = 50$ to noised image A to yield a new image A_1;
5) Perform singular value decomposition to the acquired image A_1;
6) Calculate the average of the last M singular values P_{1M};
7) Figure out the estimated noise level by Formula (28).

IV. Simulation Results

A. Performance of the Proposed Method

The proposed method was tested on various types of images. In our experiments on both cartoon and real-world gray images, we calculate PM and P1M as the average of the tail of singular values (the last 75% of singular values, i.e., $M = (3r)/4$).

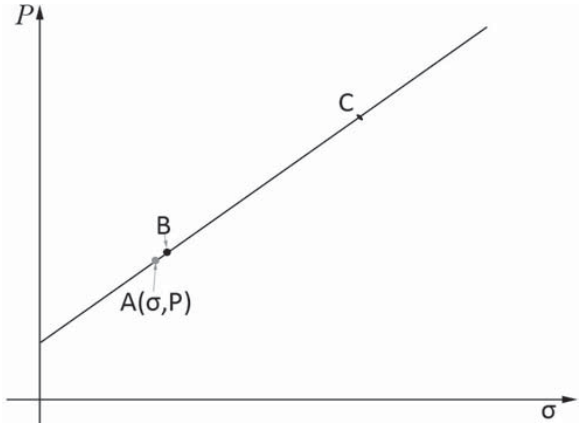

Fig. 7. Influence of σ_1.

We select some test images shown in Figure 1, the test images (a), (b), (c) are 512×512 standard grayscale images; among them (a) is an image with simple structure and less visual details, while (c) is a complicated image with lots of details; image (d) is a 256×256 standard grayscale image; images (e) and (f) are cartoons of size 256×256 and 533×512 respectively. A 256×256 blank image with gray levels equal to 127 was also included in our experiment as the "flattest" image. When drawings of cartoonists are scanned into computers, noise is inevitable, so we take cartoons into consideration in this research. All these images are selected for test in this work due to their meaningful span and variations in visual content and resolution.

Tables II and III show the statistical results from the experiment data: Table II gives the mean estimation results of 100 tests of each image with difference noising processes, while Table III gives the associated standard deviation. We test each image 100 times under a certain noise level in order to check if the proposed method can work stably. The experimental results proved that the proposed method is effective for both real-world and cartoon images, and the noise level of AWGN can be estimated reasonably well in the SVD domain. Comparing the estimate results of each image, we can also see the efficiency of our technique has little to do with the content of images. Our abundant tests show that from "flattest" image to ordinary images with details and flat areas, and to images that are rich of edges, the estimate results are of about the same accurate.

In addition, changing the value of M has little influence on the experimental result, as long as its value ranging from $\frac{r}{4}$ to $\frac{4r}{5}$. Table IV gives the experimental results on Lena (512×512) with different M values (within the range of $\left[\frac{r}{4}, \frac{4r}{5}\right]$).

B. Performance Comparisons

We have compared proposed method with 3 existing methods. Figure 8 gives the simulation results. The X axis denotes the noise level σ, and the Y denotes the noise estimation error $\delta = \hat{\sigma} - \sigma$.

Fig. 8(a) shows the comparison results with Method A which is an algorithm combining filter-based and block-based estimation algorithms proposed by Dong-Hyuk Shin and Rae-Hong Park recently [36]. It is a fast noise estimation algorithm

TABLE II
MEAN $\hat{\sigma}$ FOR 100 TESTS

Noise	$\sigma = 10$	$\sigma = 15$	$\sigma = 20$	$\sigma = 25$	$\sigma = 30$	$\sigma = 35$	$\sigma = 40$	$\sigma = 45$	$\sigma = 50$
Peppers	10.14	14.99	20.19	24.74	30.02	34.80	39.80	44.79	50.02
Lena	9.91	14.94	19.97	24.82	30.02	35.15	39.90	45.00	50.23
Barbara	9.37	14.59	19.85	25.20	30.48	35.69	40.63	45.44	50.55
Cameraman	10.50	15.24	20.13	25.03	30.12	34.94	40.00	44.93	50.15
Cartoon1	9.43	14.35	19.29	24.21	29.69	34.40	39.62	44.82	49.67
Cartoon2	10.83	14.96	19.55	24.40	29.62	34.61	39.63	44.88	49.98
Blank	9.96	15.02	19.95	24.99	29.92	35.02	40.05	45.08	49.90

TABLE III
STANDARD DEVIATION OF $\hat{\sigma}$ ESTIMATION FOR 100 TESTS

Noise	$\sigma = 10$	$\sigma = 15$	$\sigma = 20$	$\sigma = 25$	$\sigma = 30$	$\sigma = 35$	$\sigma = 40$	$\sigma = 45$	$\sigma = 50$
Peppers	0.15	0.21	0.29	0.30	0.44	0.46	0.58	0.57	0.67
Lena	0.17	0.18	0.30	0.34	0.41	0.47	0.52	0.60	0.64
Cameraman	0.19	0.23	0.26	0.34	0.36	0.51	0.67	0.69	0.81
Barbara	0.14	0.19	0.28	0.36	0.42	0.48	0.60	0.59	0.66
Cartoon1	0.14	0.21	0.27	0.34	0.47	0.47	0.55	0.62	0.65
Cartoon2	0.19	0.23	0.34	0.38	0.40	0.51	0.52	0.65	0.62
Blank	0.14	0.16	0.18	0.22	0.33	0.40	0.47	0.51	0.56

TABLE IV
ESTIMATION RESULTS WITH DIFFERENT M

Noise	$\sigma = 10$	$\sigma = 15$	$\sigma = 20$	$\sigma = 25$	$\sigma = 30$	$\sigma = 35$	$\sigma = 40$	$\sigma = 45$	$\sigma = 50$
$M = 128$	9.92	15.12	20.10	25.13	30.11	34.91	40.14	44.89	50.21
$M = 192$	9.97	14.89	19.95	25.11	30.13	35.21	40.22	45.23	50.16
$M = 256$	9.90	14.95	19.96	24.83	30.06	35.09	39.91	45.10	50.24
$M = 320$	9.87	14.89	20.16	24.84	30.07	34.90	39.87	44.99	50.13

using a Gaussian filter. In order to estimate the amount of noise, images are split into a number of blocks and smooth blocks are selected. The standard deviation of noise is computed from the difference of the selected block images between the noisy input image and its filtered image. Method A works well only when $\sigma < 15$. So we compare the estimation results in cases when $\sigma \leq 15$. The estimation results of Method A are extracted directly from [36]. We get our estimation results in Fig. 8 (a) by exactly the same test method as [36]: in experiments, the median of estimated noise standard deviations with 50 simulations for each case is our estimation result.

Fig. 8(b) gives the comparison results with two wavelet domain methods. Method B is a currently widely-used estimating method proposed by D. L. Donoho and I. M. Johnstone [23], which depends on wavelet coefficients of noisy image. The approach estimates σ as (3). We can see that this method gives good estimates for large noise cases, but overestimates the noise for small noise cases, as shown in Fig. 8(b). Method C is an up-to-date modified algorithm in wavelet domain [40]. Compared to Method B, it improves the precision of estimation in situations of low noise. We have implemented Method B and C. In our simulation, the same test procedure as [40] is performed: 1200 natural images are tested, and AGWNs of level from 10 to 50 are added to each image. The estimation results are the average estimation results of each image.

From Figure 8 we can see that the proposed method overall outperforms the most widely-used and the most up-to date existing methods, and it can estimate the noise level accurately on both smooth and detailed images.

However, the proposed method is outperformed by Method A on image Baboon when noise level is low. The reason for lower performance at low noise level is that, when noise level is low, the tail of singular values used for performing estimation may be dominated by both noise and image signal, especially for images of high activity. This will affect the estimation accuracy. One possible solution is to choose an adaptive length of the tail of singular values, so that all the chosen singular values are dominated by noise. This will be our further research.

C. Three Criteria for Noise Estimators

In [38], three criteria: accuracy, reliability and stability, are proposed for evaluating noise estimators. In terms of accuracy and reliability, [38] used the same quality measures as those suggested by Amer and Dubois [51]. Average estimation error and the average variance of estimation errors are used as the

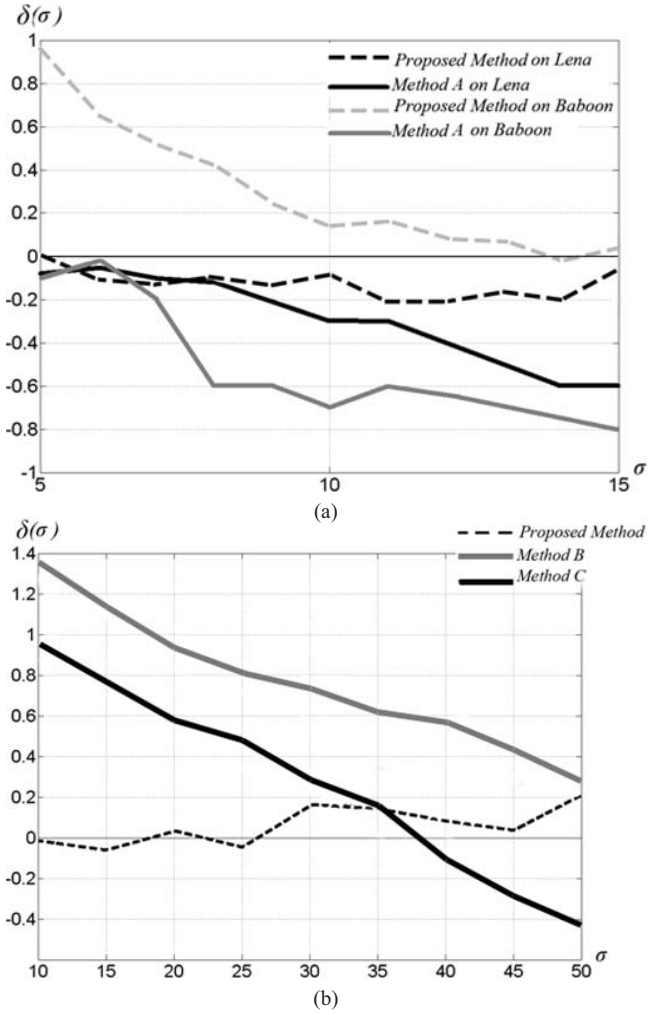

Fig. 8. Performance comparison of the noise estimation methods. (a) Comparison with Method A. (b) Comparison with Method B and C.

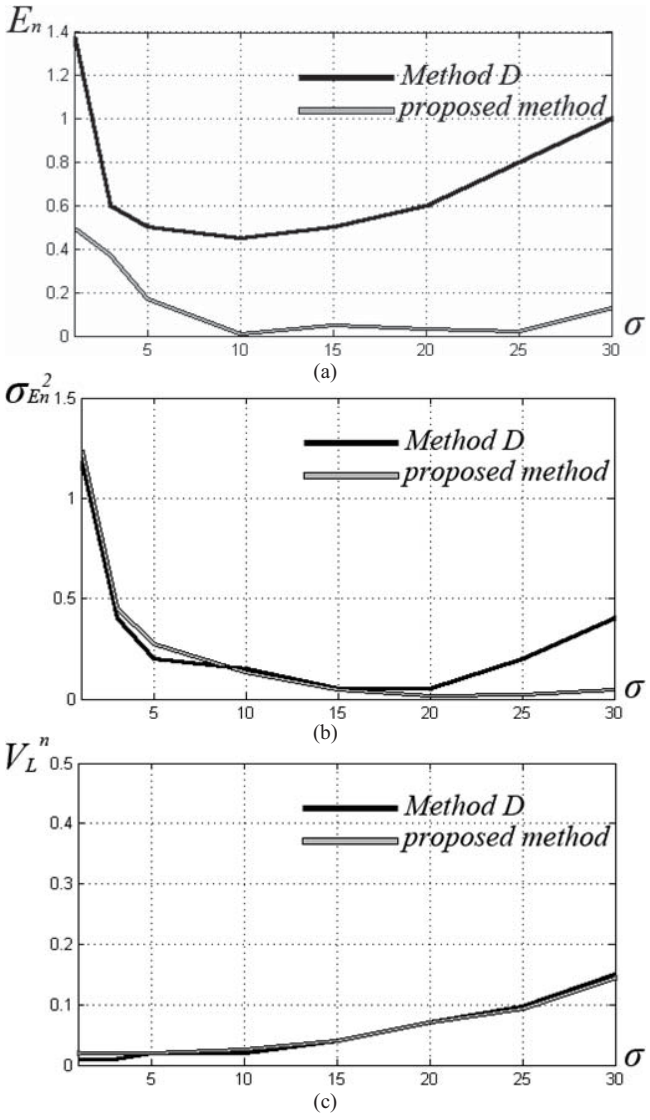

Fig. 9. Comparison based on three criteria. (a) Comparison of accuracy. (b) Comparison of reliability. (c) Comparison of stability.

measures.

$$E_{i,n} = \frac{1}{L}\sum_{l=1}^{L} |\hat{\sigma^{i,n}}(l) - \sigma^{i,n}(l)| \tag{29}$$

$$E_n = \frac{1}{N_I}\sum_{i=1}^{N_I} E_{i,n} \tag{30}$$

$$\sigma_{E_n}{}^2 = \frac{1}{N_I}\sum_{i=1}^{N_I} \left(E_{i,n} - E_n\right)^2. \tag{31}$$

In above Formulas, super- and subscripts i represent the index of the test images, and n denotes the simulated noise level. For each image at each noise level, the simulation is repeated L times and l is the index of these repetitions. NI is the total number of test images The average estimation error of the L simulations for image i at noise level n is $E_{i,n}$. The overall average estimation error at noise level n is En. For a good estimator, this value should be as small as possible. The overall average variance of estimation errors at noise level n is $\sigma_{E_n}{}^2$. For a good estimator, this value should be as small as possible.

Stability of a noise estimator means that the results should be close to each other under the same settings (e.g., the same image and the same noise level). In terms of this aspect, [38] propose the following quality measure:

$$\hat{\sigma}^{i,n} = \frac{1}{L}\sum_{l=1}^{L} \hat{\sigma}^{i,n}(l) \tag{32}$$

$$V_L^n = \frac{1}{N_I}\sum_{i=1}^{N_I}\frac{1}{L}\sum_{l=1}^{L}\left[\hat{\sigma}^{i,n}(l) - \hat{\sigma}^{i,n}\right]^2. \tag{33}$$

In above Formula, V_L^n is the overall average variance of estimated noise deviations at noise level n. For a good estimator, the value should be as small as possible.

We made performance comparisons of proposed method and the method proposed by [38] based on the three quality measures defined above; E_n and $\sigma_{E_n}{}^2$ show the accuracy and reliability of the method for different types of images, and V_L^n denotes the stability of the method. Twenty different 512×512 images are included in our simulation (including blank image,

ordinary images with details and flat areas and images rich of edges). In real-world, typical noise levels are within range 3 to 25 [38]. Therefore, we choose to run simulations at noise levels of range 1 to 30. The simulation for each image at each noise level is repeated 10 times. i.e., $L = 10$. Figure 9 shows the overall performance comparisons between Method D (the reference method in [38]) and the proposed method. 2 parameters of reference method need to be set. We choose optimal choice: $P = 10\%$ and $W_b = 5$. We can see that the proposed method achieved overall better performance. However, like most noise estimators, when noise level is lower than 10, the performance of proposed method is somewhat unsatisfying. During the procedure of estimation, the tail of singular values is used as the data basis for noise estimation, as mentioned in part I, it is dominated by noise. At low noise circumstance, the image details may be relatively strong especially for images rich of edges. As a result, the estimate results based on the tail of singular values may not be accurate and stable. That is to say, when noise level is below 10, the efficiency of our technique is related to image content, the estimation error increases for images with strong structure. We can also see this from Fig. 8(a).

D. Computation Complexity

In order to estimate noise level, we need to apply SVD to the full image twice. Therefore, the complexity of the proposed method is a very important issue. We implemented our methods on a personal computer running Windows 7 Enterprise with one 2.4 GHz Intel Core(TM)2 CPU and 2 Gbytes of main memory. The average execution time for 512×512 images is about 0.9 s. If we design parallel computer programs, the memory requirement will be double, since two images have to be stored. If serial programs are designed, we only need to prepare memory for storing one image.

Among all the estimation algorithms, block-based algorithms are the simplest with the worst estimation accuracy. The main computation of the filter-based estimation algorithm is for convolution. The standard computation time for convolving a $k \times k$ window of weighting coefficients with an $m \times n$ image is $O(m \times n \times k^2)$. The main computation of the transform-based estimation algorithm is for the transform part, i.e. DCT, DWT, SVD. The standard computation time for a DWT of an $m \times n$ matrix is $O(m \times n)$. The standard computation time for a SVD of a dense $m \times n$ matrix is $O(m \times n \times min\{m, n\})$. With the developments of fast SVD ([52], [53]), the CPU time for fast SVD can be reduced by 56$\sim$99%. Furthermore, if we tessellate the noisy image into blocks with fixed size, the computation time for block-based SVD will be *O(constant)* without jeopardizing estimation accuracy. Tessellating noisy image into blocks, applying SVD on selected blocks, and estimating noise level based on Block-SVD will be our further research for implementation efficiency. In this manuscript, we have had our emphasis on demonstrating the effective use of SVD for noise level estimation.

V. Conclusion

Singular Value Decomposition (SVD) has been a basic tool for signal processing and analysis for long, but has been less explored for noise estimation in images. In this paper, we have firstly shown how to infer the noise level according to image singular values out of SVD, due to the fact that the influence of signal and noise can be separated well in the SVD space. In addition, we have proposed to add new noise (and therefore, known noise) to images to be estimated, and analyze the change of singular values in order to determine the content related parameter in the model (so that the proposed method can be applied to any kind of images). Our simulation results show that the proposed approach outperforms the relevant existing estimation methods over a wide range of visual content and noise conditions. Experiments results demonstrated that the proposed algorithm can determine noise levels better.

Noise level estimation is useful for many computer vision and other image processing algorithms that require knowing the noise level beforehand. Examples of algorithms requiring noise level estimates include motion estimation, denoising, super-resolution, shape-from-shading, and feature extraction. Automatically inferring the image noise level and taking it into account in the algorithms that follow are important and meaningful in such algorithms and systems. The proposed and image processing algorithms better-grounded and more reliable.

Acknowledgment

The authors are grateful to the anonymous reviewers for their valuable comments and suggestions.

References

[1] C. Boncelet, *Image Noise Models*. New York: Academic, 2005.
[2] T. S. Huang, *Advances in Computer Vision and Image Processing*, Greenwich, CT: JAI Press, 1986.
[3] B. W. Keelan and R. E. Cookingham, *Handbook of Image Quality*. Boca Raton, FL: CRC Press, 2002.
[4] M. A. Covington, *Digital SLR Astrophotography*. Cambridge, U.K.: Cambridge Univ. Press, 2007.
[5] J. Ohta, *Smart CMOS Image Sensors and Applications*. Boca Raton, FL: CRC Press, 2008.
[6] R. C. Gonzalez and R. E. Woods, *Digital Image Processing*. Englewood Cliffs, NJ: Prentice-Hall, 2007.
[7] L. G. Shapiro and G. C. Stockman, *Computer Vision*. Englewood Cliffs, NJ: Prentice-Hall, 2001.
[8] J. G. Pellegrino, J. Zeibel, R. G. Driggers, and P. Perconti, *Infrared Camera Characterization*. Boca Raton, FL: CRC Press, 2006.
[9] L. MacDonald, *Digital Heritage*. London, U.K.: Butterworth, 2006.
[10] J. R. Janesick, *Scientific Charge-Coupled Devices*. Bellingham, WA: SPIE, 2001.
[11] R. E. Jacobson, S. F. Ray, G. G. Attridge, and N. R. Axford, *The Manual of Photography*. Waltham, MA: Focal Press, 2000.
[12] M. Droske and M. Rumpf, "Multiscale joint segmentation and registration of image morphology," *IEEE Trans. Pattern Anal. Mach. Intell.*, vol. 29, no. 12, pp. 2181–2194, Dec. 2007.
[13] X. Shen and C. R. Dietlein, "Detection and segmentation of concealed objects in terahertz images," *IEEE Trans. Image Process.*, vol. 17, no. 12, pp. 2465–2475, Dec. 2008.
[14] N. Zheng, Q. You, and G. Meng, "50 years of image processing and pattern recognition in China," *IEEE Intell. Syst.*, vol. 23, no. 6, pp. 33–41, Nov.–Dec. 2008.
[15] B. J. Kang and K. R. Park, "Real-time image restoration for iris recognition systems," *IEEE Trans. Syst., Man, Cybern., B, Cybern.*, vol. 37, no. 6, pp. 1555–1566, Dec. 2007.
[16] Y. Wen, M. K. Ng, and Y. Huang, "Efficient total variation minimization methods for color image restoration," *IEEE Trans. Image Process.*, vol. 17, no. 11, pp. 2081–2088, Nov. 2008.

[17] Q.-X. Tang and L.-C. Jiao, "Image denoising with geometrical thresholds," *Electron. Lett.*, vol. 45, no. 8, pp. 405–406, 2009.
[18] J. Portilla, V. Strela, M. J. Wainwright, and E. P. Simoncelli, "Image denoising using scale mixtures of Gaussians in the wavelet domain," *IEEE Trans. Image Process.*, vol. 12, no. 11, pp. 1338–1351, Nov. 2003.
[19] M. Elad and M. Aharon, "Image denoising via sparse and redundant representations over learned dictionaries," *IEEE Trans. Image Process.*, vol. 15, no. 12, pp. 3736–3745, Dec. 2006.
[20] M. Mahmoudi and G. Sapiro, "Fast image and video denoising via nonlocal means of similar neighborhoods," *IEEE Signal Process. Lett.*, vol. 12, no. 12, pp. 839–842, Dec. 2005.
[21] S. I. Olsen, "Estimation of noise in images: An evaluation," *CVGIP, Graph. Models Image Process.*, vol. 55, no. 4, pp. 319–323, 1993.
[22] G. A. Mastin, "Adaptive filters for digital image noise smoothing: An evaluation," *Comput. Vis., Graph., Image Process.*, vol. 31, no. 1, pp. 103–121, 1985.
[23] D. Donoho, "De-noising by soft-thresholding," *IEEE Trans. Inf. Theory*, vol. 41, no. 3, pp. 613–627, May 1995.
[24] S. Wu, W. Lin, S. Xie, Z. Lu, E. Ong, and S. Yao, "Blind blur assessment for vision-based applications," *J. Visual Commun. Image Represent.*, vol. 20, no. 4, pp. 231–241, May 2009.
[25] S. Baker and I. Matthews, "Lucas-Kanade 20 years on: A unifying framework," *Int. J. Compt. Vis.*, vol. 56, no. 3, pp. 221–255, 2004.
[26] W. T. Freeman, E. C. Pasztor, and O. T. Carmichael, "Learning low-level vision," *Int. J. Compt. Vis.*, vol. 40, no. 1, pp. 25–47, 2000.
[27] R. Zhang, P. Tsai, J. Cryer, and M. Shah, "Shape from shading: A survey," *IEEE Trans. Pattern Anal. Mach. Intell.*, vol. 21, no. 8, pp. 690–706, Aug. 1999.
[28] D. Lowe, "Object recognition from local scale-invariant features," in *Proc. IEEE Int. Conf. Comput. Vis.*, Dec. 1999, pp. 1150–1157.
[29] J. Nakamura, *Image Sensors and Signal Processing for Digital Still Cameras*. Boca Raton, FL: CRC Press, 2005.
[30] F. Russo, "A method for estimation and filtering of Gaussian noise in images," *IEEE Trans. Instrum. Meas.*, vol. 52, no. 4, pp. 1148–1154, Aug. 2003.
[31] K. Rank, M. Lendl, and R. Unbehauen, "Estimation of image noise variance," *Proc. IEE-Vis., Image Signal Process.*, vol. 146, no. 2, pp. 80–84, Apr. 1999.
[32] J. S. Lee, "Refined filtering of image noising using local statistics," *Comput. Graph. Image Process.*, vol. 15, no. 4, pp. 380–389, 1981.
[33] R. C. Bilcu and M. Vehvilainen, "A new method for noise estimation in images," in *Proc. IEEE EURASIP Int. Workshop Nonlinear Signal Image Process.*, Sapporo, Japan, Nov. 2005, pp. 1–25.
[34] J. Immerkær, "Fast noise variance estimation," *Comput. Vis. Image Understand.*, vol. 64, no. 2, pp. 300–302, Sep. 1996.
[35] A. Amer and E. Dubois, "Fast and reliable structure-oriented video noise estimation," *IEEE Trans. Circuits Syst. Video Technol.*, vol. 15, no. 1, pp. 113–118, Jan. 2005.
[36] D. Shin and R. Park, "Block-based noise estimation using adaptive Gaussian filtering," *IEEE Trans. Consum. Electron.*, vol. 51, no. 1, pp. 218–226, Feb. 2005.
[37] S. Tai and S. Yang, "A fast method for image noise estimation using Laplacian operator and adaptive edge detection," in *Proc. 3rd Int. Symp. Commun. Control Signal Process.*, 2008, pp. 1077–1081.
[38] S. M. Yang and S. C. Tai, "Fast and reliable image-noise estimation using a hybrid approach," *J. Electr. Imag.*, vol. 19, no. 3, p. 033007, Jul.–Sep. 2010.
[39] A. Stefano, P. White, and W. Collis, "Training methods for image noise level estimation on wavelet components," *EURASIP J. Appl. Signal Process.*, vol. 16, pp. 2400–2407, Jan. 2004.
[40] T. Li and M. Wang, "Estimating noise parameter based on the wavelet coefficients estimation of original image," in *Proc. Int. Conf. Challenges Environ. Sci. Comput. Eng.*, vol. 1. 2010, pp. 126–129.
[41] J. Mairal, M. Elad, and G. Sapiro, "Sparse representation for color image restoration," *IEEE Trans. Image Process.*, vol. 17, no. 1, pp. 53–69, Jan. 2008.
[42] M. Elad and M. Aharon, "Image denoising via sparse and redundant representations over learned dictionaries," *IEEE Trans. Image Process.*, vol. 15, no. 12, pp. 3736–3745, Dec. 2006.
[43] M. Protter and M. Elad, "Image sequence denoising via sparse and redundant representations," *IEEE Trans. Image Process.*, vol. 18, no. 1, pp. 27–35, Jan. 2009.
[44] Y. He, T. Gan, W. Chen, and H. Wang, "Adaptive denoising by singular value decomposition," *IEEE Signal Process. Lett.*, vol. 18, no. 4, pp. 215–218, Apr. 2011.
[45] M. Narwaria and W. Lin, "Objective image quality assessment based on support vector regression," *IEEE Trans. Neural Netw.*, vol. 21, no. 3, pp. 515–519, Mar. 2010.
[46] X. Zhu and P. Milanfar, "Automatic parameter selection for denoising algorithms using a no-reference measure of image content," *IEEE Trans. Image Process.*, vol. 19, no. 12, pp. 3116–3132, Dec. 2010.
[47] N. S. Kamel, S. Sayeed, and G. A. Ellis, "Glove-based approach to online signature verification," *IEEE Trans. Pattern Anal. Mach. Intell.*, vol. 30, no. 6, pp. 1109–1113, Jun. 2008.
[48] W. S. Hoge and C.-F. Westin, "Identification of translational displacements between N-dimensional data sets using the high-order SVD and phase correlation," *IEEE Trans. Image Process.*, vol. 14, no. 7, pp. 884–889, Jul. 2005.
[49] H. Zhao, P. C. Yuen, and J. T. Kwok, "A novel incremental principal component analysis and its application for face recognition," *IEEE Trans. Syst., Man, Cybern., B, Cybern.*, vol. 36, no. 4, pp. 873–886, Aug. 2006.
[50] B. Noble and L. W. Daniel, *Applied Linear Algebra*. Englewood Cliffs, NJ: Prentice-Hall, 1988.
[51] A. Amer and E. Dubois, "Fast and reliable structure-oriented video noise estimation," *IEEE Trans. Circuits Syst. Video Technol.*, vol. 15, no. 1, pp. 113–118, Jan. 2005.
[52] A. K. Menon and C. Elkan, "Fast algorithms for approximating the singular value decomposition," *ACM Trans. Knowl. Discovery Data*, vol. 5, no. 2, pp. 1–36, Feb. 2011.
[53] C. Zhan, K. Jheng, and Y. Chen, "High-convergence-speed low-computation-complexity SVD algorithm for MIMO-OFDM systems," in *Proc. IEEE Int. Symp. VLSI Design, Autom. Test*, Dec. 2009, pp. 195–198.

Wei Liu was born in Hunan, China, in 1976. She received the B.S. degree from the Huazhong University of Science and Technology, Wuhan, China, in 1997, and the Ph.D. degree from Sun Yat-Sen University, Guangzhou, China, in 2005, both in electronic engineering.

She is currently involved in teaching and research with the School of Computer Science, South China Normal University, Guangzhou. Her current research interests include image and video signal processing.

Weisi Lin (M'92–SM'98) received the B.Sc. degree in electronics and the M.Sc. degree in digital signal processing from Zhongshan University, Guangzhou, China, in 1982 and 1985, respectively, and the Ph.D. degree in computer vision from King's College, London University, London, U.K., in 1992.

He was involved in teaching and research with Zhongshan University, Shantou University, Shantou, China, Bath University, Bath, U.K., the National University of Singapore, the Institute of Microelectronics, Singapore, and the Institute for Infocomm Research, Singapore. He has been the project leader of 13 major successful projects in digital multimedia technology development. He was the Laboratory Head of Visual Processing and the Acting Department Manager of Media Processing, Institute for Infocomm Research. He is currently an Associate Professor with the School of Computer Engineering, Nanyang Technological University, Singapore. His current research interests include image processing, perceptual modeling, video compression, multimedia communication, and computer vision.